Solar Cells

DOI: 10.1002/anie.201104102

High-Performance Silicon Nanowire Array Photoelectrochemical Solar Cells through Surface Passivation and Modification**

Xin Wang, Kui-Qing Peng, Xiao-Jun Pan, Xue Chen, Yang Yang, Li Li, Xiang-Min Meng, Wen-Jun Zhang, and Shuit-Tong Lee**

Direct conversion of sunlight to electricity by means of photovoltaic (PV) technology can play an important role in addressing the global energy crisis. Currently, 90% of commercial PV modules manufactured worldwide are made of solar-grade Si owing to its high natural abundance, mature processing technology, and excellent reliability in solar cells.[1] However, the widespread implementation of Si PVs is limited by the high-cost production of solar-grade Si wafer. Many approaches have been taken to lower the production cost of Si PVs, among which thin-film Si solar cells offer a promising low-cost solution;[2,3] however, thin-film Si solar cells have lower efficiencies than bulk Si, due to their limited absorption thickness. In recent years, solar cells based on silicon nanowires (SiNWs) have attracted great interest because of their potential for high conversion efficiency at low cost.[4–31] In particular, SiNWs prepared by metal-catalyzed electroless etching (MCEE) are under investigation as components for solar cells.[16–31] As a prototypical system to explore new concepts for solar energy conversion, liquid-junction SiNW photoelectrochemical solar cells (PECs) have attracted intense attention in the past years,[26–30] and the potential of MCEE SiNWs for solar energy conversion were further highlighted by Wang et al.[31] The MCEE SiNWs with high surface roughness would benefit thermoelectric applications,[32] but suffer from undesirable recombination losses and photocorrosion, resulting in low efficiencies and rapid performance degradation of PECs. Hence, reducing recombination losses and photocorrosion by surface passivation is crucial for the realization of high-performance SiNW PECs, which, however, remain largely unexplored.

Here we address the issues of surface passivation and performance degradation associated with SiNWs PECs. We report a novel design of platinum nanoparticle (PtNP)-decorated carbon/silicon core/shell nanowire (PtNPs@C@SiNW) arrays for high-performance PECs. Ultrathin carbon film was coated onto SiNWs to form a core/shell structure, followed by decoration with PtNPs. In this hybrid architecture, the environmentally friendly and chemically stable carbon film passivates the SiNW surfaces and protects them against photocorrosion, while the PtNPs further improve the stability of SiNWs and lead to a significant increase in power-conversion efficiency owing to enhanced interfacial charge transfer. The resultant PtNPs@C@SiNW array exhibits a power-conversion efficiency of up to 10.86% and excellent performance stability in aggressive aqueous HBr/Br_2 electrolyte under 1-sun AM 1.5G illumination.

Fabrication of the PtNPs@C@SiNW array is illustrated in Figure 1. First, vertically aligned n-SiNW arrays were prepared on n-Si(100) wafer by the MCEE method, as described previously.[33,34] The SiNW samples were washed with deionized water and then immersed in a bath of concentrated nitric acid for 30 min to remove Ag from the SiNW surfaces. After removing the oxide layer with buffered hydrofluoric acid solution, a thin carbon coating was applied by MPECVD with CH_4/10% H_2 at 500 °C and 12 Torr, that is, conditions under which conformal surface deposition is achieved. The thickness of carbon film is controlled by the MPECVD time. PtNPs were selectively deposited onto SiNW surfaces through pinholes in the carbon coating by electroless metal deposition (EMD) in a solution containing 50:1 H_2O:HF solution and K_2PtCl_6 (0.001 M).

Figure 2a shows a cross-sectional SEM image of PtNPs@C@SiNW the array. The nanowire length is about 10 μm, and the diameter is in the range of 30–300 nm. The C/Si core/shell structure can be distinctly identified in the high-resolution TEM (HRTEM) image. A HRTEM image taken near the edge of one nanowire shows the single-crystal structure of the silicon core and the thin shell layer with a thickness of about 2 nm (Figure 2b). Electron energy-loss spectroscopy (EELS) at the core/shell interface region reveals the presence of Si and C, and confirms that the composition of the shell layer is C. Figure 2d shows an HRTEM image of PtNPs@C@SiNW, and NPs with a diameter of 5–10 nm. Energy-dispersive spectroscopy (EDS) analysis on a small area covering PtNPs (Figure 2e) showed dominant Si, C, and Pt signals, and little oxygen signal, that is little Si oxide remains.

[*] X. Wang, Prof. K.-Q. Peng, L. Li
Department of Physics and College of Nuclear Science and Technology
Beijing Normal University, Beijing 100875 (China)
E-mail: kq_peng@bnu.edu.cn
X. J. Pan, Y. Yang, Prof. W. J. Zhang, Prof. S.-T. Lee
Center of Super-Diamond and Advanced Films (COSDAF) and Department of Physics and Materials Science
City University of Hong Kong, Hong Kong SAR (China)
E-mail: apannale@cityu.edu.hk
X. Chen, Prof. X. M. Meng
Technical Institute of Physics and Chemistry
Chinese Academy of Sciences CAS (China)

[**] This work is supported by the NSFC (51072025, 50702010), Beijing Natural Science Foundation (2112021), National Basic Research Program of China (2012CB932400), National Excellent Doctoral Dissertations of China (200743), NCET-08–0060, Beijing Nova Program (2008B24), Fok Ying Tung Education Foundation (121047), and Research Grants Council of Hong Kong SAR (CityU5/CRF/08 and CityU101909).

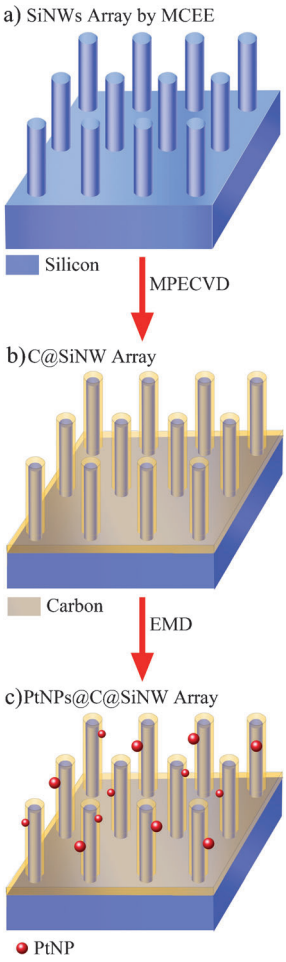

Figure 1. Schematic illustration of the fabrication process of a PtNPs@C@SiNW array. a) SiNW array prepared by the MCEE method. b) C/Si core/shell nanowire array after carbon MPECVD. c) PtNPs@C@SiNW array after PtNP EMD.

The diffuse reflectance of the prepared samples was measured on a UV/Vis/NIR spectrophotometer equipped with an integrating sphere. The average reflectance of the PtNPs@C@SiNW array of about 2.0% in the wavelength range of 300–1050 nm (Figure 3) indicates excellent light-trapping ability of MCEE SiNWs, as previously reported. This remarkably low broadband reflectance is a major advantage of cost-effective SiNW-based solar cells.

The minority carrier lifetime in Si materials is one of the key parameters affecting the performance of Si solar cells. A Semilab WT-1000 microwave photoconductive decay (μ-PCD) system was used to measure the minority carrier lifetimes of the samples. Figure 4 shows the lifetimes of SiNW samples after different surface treatments. The lifetime of the original polished Si wafer was 18.12 μs, which decreased to about 10 μs after formation of SiNW arrays. After 5 min of immersion in dilute aqueous HF solution, the lifetime of the resultant H-passivated SiNWs increased to 14 μs. Significantly, the pronounced surface-recombination effect in the SiNW samples can be substantially mitigated by deposition of a conformal carbon layer, as C@SiNW array samples show improvement in lifetime to as high as 21 μs. Owing to the additional surface defects accompanying PtNP deposition, the lifetime of the PtNPs@C@SiNW array decreased to 18.45 μs, which nevertheless is still higher than that of polished Si. The improvement in lifetime indicates that the carbon coating has an excellent surface-passivating effect on SiNWs. Furthermore, carbon is environmentally friendly and is highly stable to hostile environments, such as aggressive chemicals, and under irradiation. Therefore, the use of conformal carbon coating is an alternative promising passivation scheme for SiNWs PECs.

The effect of carbon passivation and the potential of PtNPs@C@SiNWs for PECs were investigated in an aggressive electrolyte consisting of 8.6 M hydrogen bromide and 0.05 M bromine under 1-sun AM 1.5G illumination. Figure 5a shows the representative photocurrent density–potential behavior of PtNPs@C@SiNWs in the dark and under illumination. The cell shows typical diode behavior. Under 1-sun AM 1.5G illumination, the cell exhibits an open-circuit voltage V_{oc} of 530 mV, a short-circuit current density I_{sc} of up to 36.89 mA cm^{-2}, and a fill factor (FF) of 0.555, which yield an efficiency η of 10.86%. Figure 5b shows the variation of photocurrent density with potential for different SiNW PECs after 1 h of illumination in the aggressive electrolyte. It shows that the initial output characteristics of the naked n-SiNWs PECs are poor, with low photocurrent and small fill factor, and suffer from rapid and nearly complete degradation owing to surface photooxidation during illumination. While PtNPs@SiNWs PECs showed better stability than naked n-SiNWs PECs, its initial efficiency of nearly 11% decreased to less than 5% after 1 h of light illumination. In sharp contrast, the PtNPs@C@SiNWs PECs remained at greater than 95% of the initial efficiency, that is, the presence of a conformal carbon shell can substantially stabilize the output characteristics of SiNWs PECs. Figure 5c shows the short-circuit photocurrent densities of different SiNW PECs as a function of illumination time. The results show that the stability of PtNPs@C@SiNWs in the aggressive HBr/Br_2 solution is superior. The naked H-SiNWs so extremely vulnerable to photooxidation that the photocurrent dropped quickly in the first few minutes, and decreased to nearly zero from the initial 9 mA cm^{-2} after 4 h of light illumination. In the presence of PtNPs, the photocurrent of PtNPs@SiNWs stabilized after an initial rapid decay, but lost more than 80% of its initial value after 10 h illumination, as the aggressive electrolyte oxidized the Si underneath PtNPs, and led to a substantial change in device resistance. As expected, the carbon overlayer can efficiently protect SiNWs against oxidation and corrosion. PtNPs@C@SiNWs showed less than 28% reduction in photocurrent after 10 h of illumination, and became stable afterwards. The observed reduction in photocurrent is attributable to the material quality of PtNPs@C@SiNWs. We anticipate that device performance may be further improved via optimal preparation of SiNWs, carbon overlayer, and PtNPs.

In conclusion, we have investigated the photoelectrochemical photovoltaic properties of heterostructured PtNPs@C@SiNWs, which exhibited high power conversion efficiency of 10.86% and excellent operational stability in aggressive aqueous HBr/Br_2 electrolyte under 1-sun AM 1.5G illumination. Comparison of minority carrier lifetimes, photo-

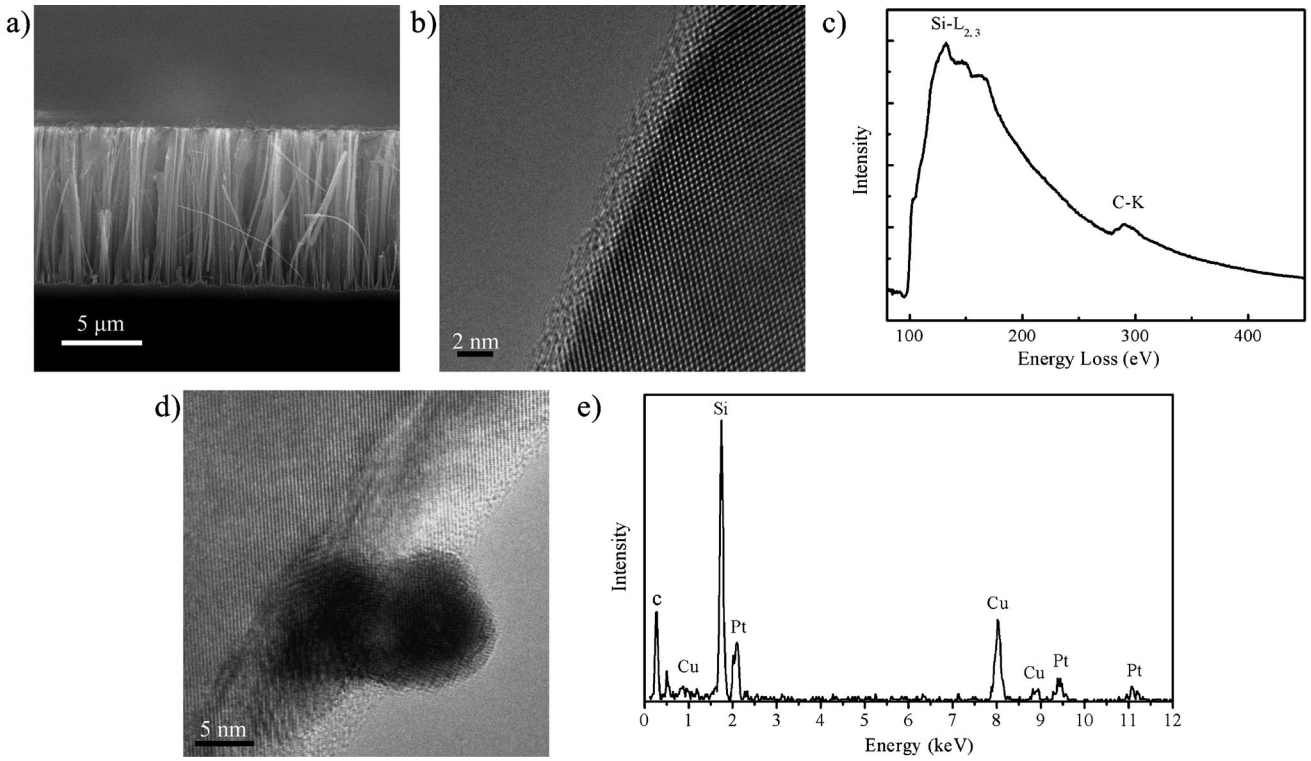

Figure 2. a) Cross-sectional SEM image of a PtNPs@C@SiNW array. b) HRTEM image of the edge of a C/Si core/shell nanowire showing ultrathin carbon shell. c) EELS spectrum recorded from the C/Si interface region. d) HRTEM image of a PtNPs@C@Si nanowire. e) EDS spectrum recorded on a small area covering PtNPs.

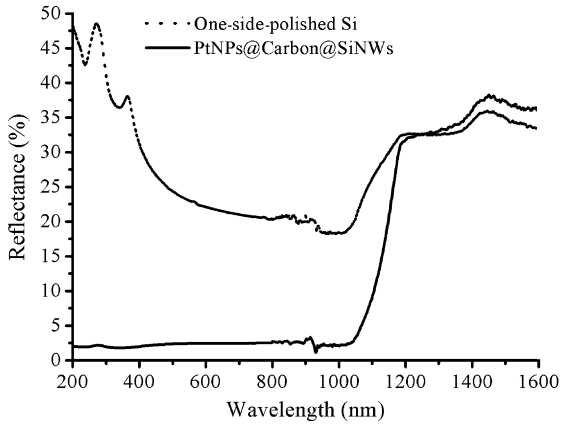

Figure 3. Hemispherical reflectance measurement of a PtNPs@C@SiNW array. As a reference, a one-side-polished single-crystal Si wafer was included.

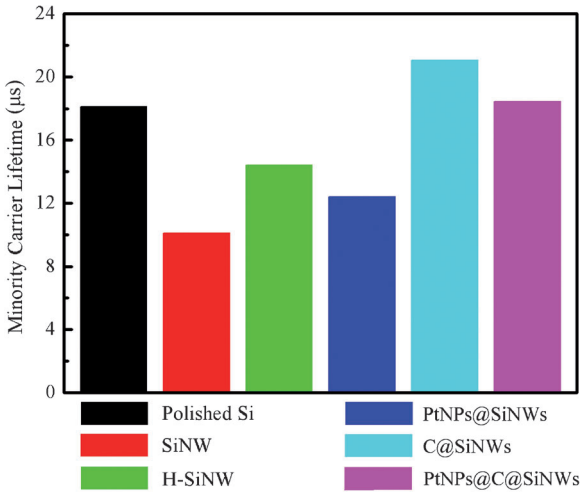

Figure 4. Minority-carrier lifetimes in samples after different surface treatments.

voltaic output characteristics, and time-dependent photocurrent density of SiNWs samples showed that carbon coating is a highly effective means of passivating SiNW surfaces, and PtNPs can significantly enhance interfacial charge transfer. Consequently, PtNPs@C@SiNW arrays are highly promising for high-performance PECs. We anticipate further improvement in cell performance may be achieved through well-tailored hetero-interfaces on SiNW surfaces, as well as optimal cell design and electrolyte, to give SiNW-based PECs with even higher performance.

Experimental Section

Fabrication of SiNWs and PtNPs@C/SiNW arrays: Single-crystal, 2–4 Ω cm n-Si(100) wafer pieces were ultrasonically degreased in acetone and ethanol at room temperature for 10 and 5 min, respectively. Then the Si wafer pieces were cleaned in boiling H_2SO_4:H_2O_2 (3:1) for about 30 min, followed by rinsing with excess copious deionized water. The cleaned Si pieces were immediately immersed in HF/$AgNO_3$ solution in sealed vessels, and vertically aligned SiNWs were produced after 30–60 min. The solution concentrations of HF and $AgNO_3$ were 5 and 0.02 mol L^{-1}, respectively. The

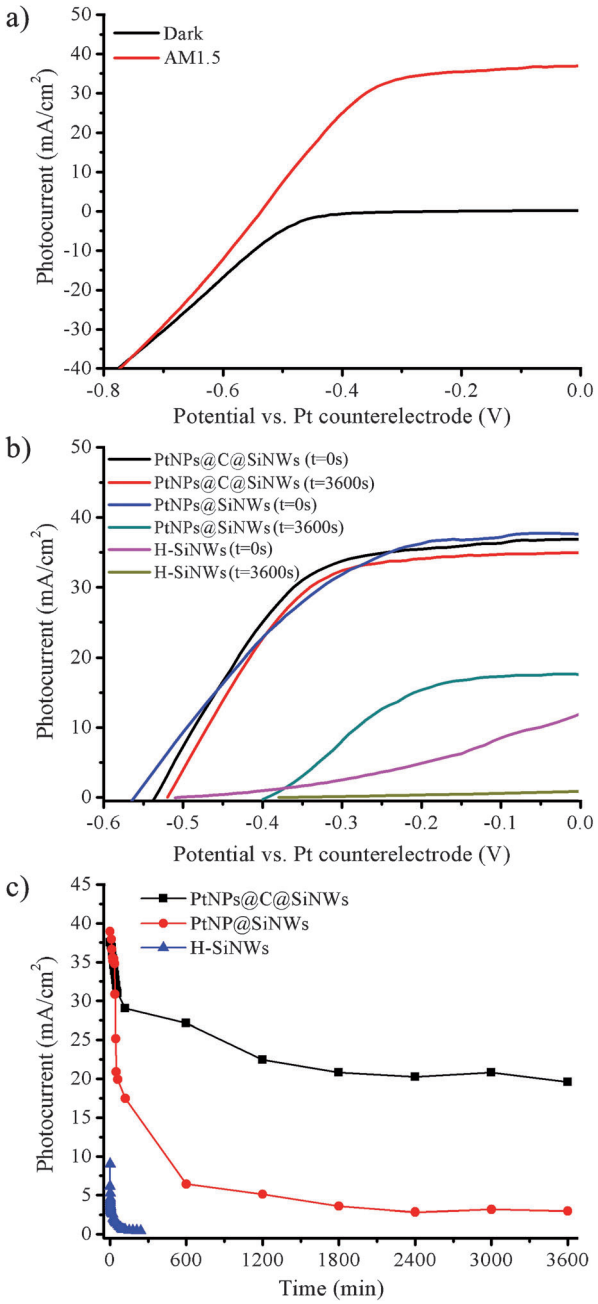

Figure 5. a) Photocurrent versus potential of PtNPs@C@SiNWs in the dark and under AM 1.5G illumination. b) Photocurrent versus potential of H-SiNWs, PtNPs@SiNWs, and PtNPs@C@SiNWs under continuous light illumination. c) Photocurrent densities of H-SiNWs, PtNPs@SiNWs, and PtNPs@C@SiNWs as a function of measurement time.

SiNW arrays were immersed in a bath of concentrated nitric acid for at least 30 min to remove residual Ag. After removing the oxide layer with buffered hydrofluoric acid solution and blowing dry the SiNWs sample with nitrogen, a conductive carbon thin film was uniformly deposited on the SiNW surfaces by microwave plasma-enhanced chemical vapor deposition (MPECVD) with CH_4/H_2 plasma and trimethylborane. The SiNW substrates were maintained at about 500 °C while the total pressure in the chamber was 12 Torr during deposition. PtNPs were deposited onto SiNWs surfaces by electroless metal deposition (EMD) in a solution containing 50:1 H_2O:HF solution and K_2PtCl_6 (0.001 M). The PtNP-decorated n-SiNW array was prepared under the same deposition conditions. The SiNWs were characterized with a Philips XL 30 FEG scanning electron microscope and a JEOL 2010F FEG transmission electron microscope equipped with energy-dispersive X-ray spectrometer. The diffuse reflectance of the samples was measured at room temperature by using a UV/VIS/NIR spectrophotometer fitted with a 150 mm integrating sphere. The minority carrier lifetimes of the samples were measured by microwave photoconductance (Semilab WT-1000)

Photoelectrochemical measurements: The photovoltaic characteristics of the as-prepared n-SiNWs were measured in an aqueous electrolyte consisting of 8.6 M hydrogen bromide and 0.05 M bromine under 1-sun AM 1.5G illumination by using an Oriel solar simulator. A two-electrode cell was used. Ti/Pd/Ag was evaporated onto the back surface of n-SiNWs electrodes to form an Ohmic contact, and then the SiNWs sample as working electrode was attached to the PEC cell with an O-ring in the form of a window. The counterelectrode was a Pt mesh. All photoelectrochemical measurements were conducted with a Princeton 2273 electrochemical workstation.

Received: June 15, 2011
Published online: September 9, 2011

Keywords: nanostructures · platinum · silicon · solar cells · surface passivation

[1] D. M. Bagnall, M. Boreland, *Energy Policy* **2008**, *36*, 4390 – 4396.
[2] M. A. Green, *Sol. Energy* **2004**, *76*, 3 – 8.
[3] J. Yoon, A. J. Baca, S. I. Park, P. Elvikis, J. B. Geddes III, L. Li, R. H. Kim, J. Xiao, S. Wang, T. H. Kim, M. J. Motala, B. Y. Ahn, E. Duoss, J. A. Lewis, R. G. Nuzzo, P. M. Ferreira, Y. Huang, A. Rockett, J. A. Rogers, *Nat. Mater.* **2008**, *7*, 907 – 915.
[4] B. Z. Tian, X. L. Zheng, T. J. Kempa, Y. Fang, N. F. Yu, G. H. Yu, J. L. Huang, C. M. Lieber, *Nature* **2007**, *449*, 885 – 888.
[5] L. Tsakalakos, J. Balch, J. Fronheiser, B. A. Korevaar, O. Sulima, J. Rand, *Appl. Phys. Lett.* **2007**, *91*, 233117.
[6] L. Hu, G. Chen, *Nano Lett.* **2007**, *7*, 3249 – 3252.
[7] T. J. Kempa, B. Z. Tian, D. R. Kim, J. S. Hu, X. L. Zheng, C. M. Lieber, *Nano Lett.* **2008**, *8*, 3456 – 3460.
[8] T. Stelzner, M. Pietsch, G. Andra, F. Falk, E. Ose, S. Christiansen, *Nanotechnology* **2008**, *19*, 295203.
[9] A. P. Goodey, S. M. Eichfeld, K. Lew, J. M. Redwing, T. E. Mallouk, *J. Am. Chem. Soc.* **2007**, *129*, 12344 – 12345.
[10] O. Gunawan, S. Guha, *Sol. Energy Mater. Sol. Cells* **2009**, *93*, 1388 – 1393.
[11] G. B. Yuan, H. Z. Zhao, X. H. Liu, Z. S. Hasanali, Y. Zou, A. Levine, D. W. Wang, *Angew. Chem.* **2009**, *121*, 9860 – 9864; *Angew. Chem. Int. Ed.* **2009**, *48*, 9680 – 9684.
[12] A. Levine, G. B. Yuan, J. Xie, D. W. Wang, *Sci. Adv. Mater.* **2010**, *2*, 463 – 473.
[13] E. Garnett, P. D. Yang, *Nano Lett.* **2010**, *10*, 1082 – 1087.
[14] A. I. Hochbaum, P. D. Yang, *Chem. Rev.* **2010**, *110*, 527 – 546.
[15] K. Q. Peng, S. T. Lee, *Adv. Mater.* **2011**, *23*, 198 – 215.
[16] K. Q. Peng, Y. Xu, Y. Wu, Y. J. Yan, S. T. Lee, J. Zhu, *Small* **2005**, *1*, 1062 – 1067.
[17] L. Tsakalakos, J. Balch, J. Fronheiser, B. A. Korevaar, O. Sulima, J. Rand, A. D. Kumar, U. Rapol, *J. Nanophotonics* **2007**, *1*, 013552.
[18] H. Fang, X. D. Li, S. Song, Y. Xu, J. Zhu, *Nanotechnology* **2008**, *19*, 255703.
[19] E. C. Garnett, P. D. Yang, *J. Am. Chem. Soc.* **2008**, *130*, 9224 – 9225.
[20] V. Sivakov, G. Andr, A. Gawlik, A. Berger, J. Plentz, F. Falk, S. H. Christiansen, *Nano Lett.* **2009**, *9*, 1549 – 1554.
[21] J. S. Huang, C. Y. Hsiao, S. J. Syu, J. J. Chao, C. F. Lin, *Sol. Energy Mater. Sol. Cells* **2009**, *93*, 621 – 624.

[22] Y. J. Hwang, A. Boukai, P. D. Yang, *Nano Lett.* **2009**, *9*, 410 – 415.
[23] S. C. Shiu, J. J. Chao, S. C. Hung, C. L. Yeh, C. F. Lin, *Chem. Mater.* **2010**, *22*, 3108 – 3113.
[24] X. Shen, B. Sun, F. Yan, J. Zhao, F. Zhang, S. Wang, X. Zhu, S. T. Lee, *ACS Nano* **2010**, *4*, 5869 – 5876.
[25] L. Wen, X. Liu, N. Yang, J. Zhai, C. Huang, Y. Li, L. Jiang, *Appl. Phys. Lett.* **2010**, *97*, 253111.
[26] K. Q. Peng, X. Wang, S. T. Lee, *Appl. Phys. Lett.* **2008**, *92*, 163103.
[27] K. Q. Peng, X. Wang, X. L. Wu, S. T. Lee, *Nano Lett.* **2009**, *9*, 3704 – 3709.
[28] E. A. Dalchiele, F. Martin, D. Leinen, R. E. Marotti, J. R. Ramos-Barrado, *J. Electrochem. Soc.* **2009**, *156*, K77 – K81.
[29] Q. K. Shu, J. Q. Wei, K. L. Wang, H. W. Zhu, Z. Li, Y. Jia, X. C. Gui, N. Guo, X. Li, C. Ma, D. H. Wu, *Nano Lett.* **2009**, *9*, 4338 – 4342.
[30] G. F. Fan, H. W. Zhu, K. L. Wang, J. Q. Wei, X. Li, Q. K. Shu, N. Guo, D. H. Wu, *ACS Appl. Mater. Interfaces* **2011**, *3*, 721 – 725.
[31] G. B. Yuan, K. Aruda, S. Zhou, A. Levine, J. Xie, D. W. Wang, *Angew. Chem.* **2011**, *123*, 2382 – 2386; *Angew. Chem. Int. Ed.* **2011**, *50*, 2334 – 2338.
[32] A. I. Hochbaum, R. Chen, R. D. Delgado, W. Liang, E. C. Garnett, M. Najarian, A. Majumdar, P. Yang, *Nature* **2008**, *451*, 163 – 166.
[33] K. Q. Peng, Y. J. Yan, S. P. Gao, J. Zhu, *Adv. Mater.* **2002**, *14*, 1164 – 1167.
[34] K. Q. Peng, Y. J. Yan, S. P. Gao, J. Zhu, *Adv. Funct. Mater.* **2003**, *13*, 127 – 132.

